Advances in Applied Sciences
2018; 3(3): 34-42
http://www.sciencepublishinggroup.com/j/aas
doi: 10.11648/j.aas.20180303.13
ISSN: 2575-2065 (Print); ISSN: 2575-1514 (Online)

Analytical Solutions of an MHD Heat and Mass Transfer of a Jeffery Fluid Flow over a Stretching Sheet with the Effect of Slip Velocity

Adamu Gizachew*, Bandari Shankar

Department of Mathematics, College of Science, Osmania University, Hyderabad, India

Email address:
adamu.giz@gmail.com (A. Gizachew)

*Corresponding author

To cite this article:
Adamu Gizachew, Bandari Shankar. Analytical Solutions of an MHD Heat and Mass Transfer of a Jeffery Fluid Flow over a Stretching Sheet with the Effect of Slip Velocity. *Advances in Applied Sciences*. Vol. 3, No. 3, 2018, pp. 34-42. doi: 10.11648/j.aas.20180303.13

Received: July 19, 2018; **Accepted**: August 13, 2018; **Published**: September 6, 2018

Abstract: In this study, we have developed an analytic model to analyze the influence of velocity slip parameter and heat source on magneto hydrodynamics (MHD) heat and mass transfer of a Jeffery fluid which conducts electricity on a stretching surface. Both temperature and concentration are assumed to be in power low form. The existing partial differential equations (PDEs) is changed into a structure of ordinary differential equations (ODE's) by using a similarity variable. For computing the transformed equation, we used an analytical method named as Optimal Homotopy Asymptotic Method (OHAM). The influence of different dimensionless parameters on the velocity, temperature, concentration and as well as the coefficient of skin friction, Nusselt number and Sherwood number were evaluated using graphs and tables. It is observed that the velocity slip parameter (k) and the Deborah number (β) have opposite effects on the velocity distributions of the fluid flow. However, the effects of heat source parameter (δ) and thermal radiation parameter (R) on the temperature profile is similar. To be confident about the accuracy of this analytic method, the values of Nusselt number (Mu_x) solved numerically is compared with the previously published works done before and the comparison is found to be in a very good agreement.

Keywords: Stretching Sheet, Slip Parameter, Heat Source, Thermal Radiation, Chemical Reaction, OHAM

1. Introduction

The flow of non-Newtonian fluid with magnetic field towards a stretching sheet has pulled in the attitude of many investigators for the last decades. Because this flow has many applications in the area of industry and manufacturing processes. Thermo-fluid problems are very much required for the production of glass fiber/plastic because these fluids are significant for the involvement of heat transfer between the surrounding fluid and sheet. Sheet process production begins by solidifying molten polymers as soon as it exists from the slit die. Immediately the sheet is solidified, it will be composed by a wind-up roll. The mechanical properties of the fiber/plastic sheet can be improved by extending rate of cooling and length of the sheet. The impression of boundary layer flow on a continuous solid sheet was launched by Sakiadis [1]. Later on, Crane [2] carried out his analysis on the mentioned kinds of flow for the case of a viscous fluid on a linearly stretching plane. Further, Crane's work have been extended by a number of investigators by considering different parameters, Dutta et al. [3], Gupta and Gupta [4], Chen and Char [5] were some of the researchers who extended it.

Most of the studies considered previously are restricted to linear stretching of the sheet. But, it is compulsory to mention that the stretching need not essentially be linear. Salleh et al. [6] examined a steady boundary layer fluid flow and the behavior of heat transfer on a stretching sheet with Newtonian heating. Similarly, a two-dimensional steady MHD fluid flow on a shrinking sheet with suction effect was investigated by Babu et al. [7]. They observed that an increase of the Hartmann number, mass suction parameter, Schmidt number, and chemical reaction parameter makes to decrease the concentration profile. Akbar et al. [8] explored stagnation point flow in the two-dimensional flow of an incompressible nanofluid towards a stretching plane with

convective boundary condition. Recently, Rout et al. [9] analyzed an electrically conducting nanofluid due to a heated stretching sheet and the transfer properties of heat and mass. They obtained that, due to higher values of radiation the heat transport rate raises, however, Sherwood number decreases. Stagnation point flows on an MHD Prandtl fluid model due to a shrinking sheet was scrutinized by Akbar et al. [10].

Radiation effect of a water-based nanofluid flow on a boundary layer near a Stagnation point with variable viscosity due to a heated convective stretching sheet was observed by Makinde and Mishra [11]. Later on, a two-dimensional MHD flow of nanofluids on a stretching plate by the cause of radiation, velocity, and thermal slip boundary conditions was investigated by Pal and Mandal [12]. A flow on a boundary layer and heat transport properties under the impact of slip velocity, Brownian motion, and thermal radiation were considered by Pal and Roy [13]. Their results have shown that the effect of slip velocity is to reduce the shear stress at the surface of the stretching sheet. Furthermore, an electrically conducting MHD flow of a nanofluid over a shrinking/stretching sheet was theoretically studied by Daniel et al. [14]. MHD viscous and heat transfer flow between two horizontal planes in a rotating system using HAM were analyzed by Sheikholeslam et al. [15].

All the studies examined by most researchers are restricted to Newtonian fluid flows. So, it is advisable to consider non-Newtonian fluid flows in the next study. Since it is very significant for several industrial and engineering applications to the flexibility of fluid characteristics in nature. Jeffery model is the simplest types of the non-Newtonian fluid model that takes into account for rheological effects of viscoelastic fluids. Because a Jeffery model is a simple linear model comparing with other models using the time derivatives instead of convective derivatives. More recently, a steady laminar MHD flow of non-Newtonian viscoelastic fluid on a horizontal expanded plane was investigated by Gizachew and Shankar [16]. Their result indicated that the thermal boundary layer thickness raises when the size of the viscoelastic parameter and magnetic field parameter increases. Moreover, Narayana and Babu [17] examined the MHD flow of an electrically conducting Jeffery fluid due to a stretching sheet with an effect of heat sink/source and chemical reaction. Their analysis showed that the Deborah number and Prandtl number has a similar effect on the Nusselt number. Recently, boundary layer flow of a mixed convection Jeffery fluid over a stretched sheet was studied by Ahmad and Ishak [18]. Further, the transfer properties of heat and mass of a Jeffery fluid with heat source/sink were investigated by Qasim [19]. The result obtained by him indicated that a Deborah number has an opposite effect on velocity and temperature distributions. The MHD flow of an electrically conducting Jeffery fluid near a stagnation point with the effect of partial slip, melting, and radiation on a stretched sheet was examined by Das et al. [20]. Furthermore, Jeffery fluid flow on a linearly stretching sheet with magnetic dipole effect was investigated by Zeeshan and Majeed [21]. More detailed studies on a Jeffery fluid model for different geometries are discussed in the following references [22–26].

Basically, this study concentrates to analyze different parameter effects on an MHD Jeffery fluid flow with heat source/sink and thermal radiation. For solving the governing problem after transformation, we used an analytic method named Optimal Homotopy Asymptotic Method (OHAM) which was developed by Marinca et al. [27]. The results obtained are shown by using graphs and tables.

2. Mathematical Formulations

In this study, we considered a steady two-dimensional incompressible, and electrically conducting Jeffery fluid flow over a linearly stretching sheet with the effect of velocity slip parameter, heat source, thermal radiation, and chemical reaction. In the physical model, the origin is fixed as it is shown in Figure 1.The flow model is located in the direction of $x-$axis and normal to the $y-$axis and this flow is produced by the exploit of two equal and opposite forces along the axis on a linear stretched sheet. In the way of flow, it is applied a consistent magnetic field of strength B_0. A fixed distance from the origin, the temperature and species concentration are considered to have power index m variations.

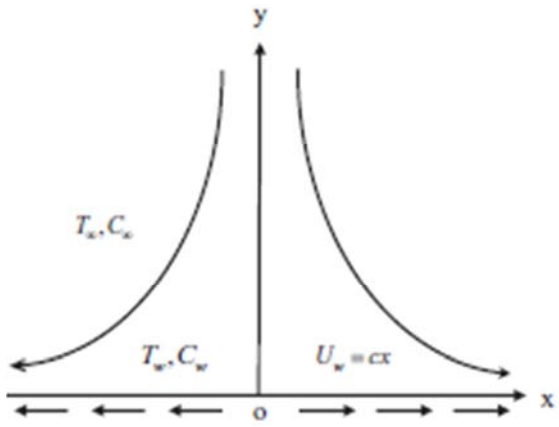

Figure 1. *Schematic diagram of the physical model and coordinate system.*

The required Jeffery fluid equation as it is developed by [23] can be written as

$$\tau = -PI + S$$

$$S = \frac{\mu}{\alpha}\left[R_1 + \lambda_1\left(\frac{\partial R_1}{\partial t} + V.\nabla\right)R_1\right]$$

The stress tensor of Cauchy, the dynamic viscosity, the Rivlin-Erickson tensor, the extra stress tensor are denoted by τ, μ , $R_1,$ and S respectively, α and λ_1 are the material parameters of Jeffery fluid.

$$R_1 = (\nabla V) + (\nabla V)^t$$

Under the above assumptions, the governing equation of continuity, momentum, energy, and conservation of mass is defined in the following form as it is developed by [28–30].

$$\frac{\partial u}{\partial x}+\frac{\partial v}{\partial y}=0 \quad (1)$$

$$u\frac{\partial u}{\partial x}+v\frac{\partial u}{\partial y}=\frac{\nu}{1+\alpha}\left[\frac{\partial^2 u}{\partial y^2}+\lambda_1\left(u\frac{\partial^3 u}{\partial x\partial y^2}+v\frac{\partial^3 u}{\partial y^3}-\frac{\partial u}{\partial x}\frac{\partial^2 u}{\partial y^2}+\frac{\partial u}{\partial y}\frac{\partial^2 u}{\partial x\partial y}\right)\right]-\frac{\sigma {B_0}^2}{\rho}u \quad (2)$$

$$u\frac{\partial T}{\partial x}+v\frac{\partial T}{\partial y}=\frac{k_f}{\rho c_p}\frac{\partial^2 T}{\partial y^2}-\frac{1}{\rho c_p}\frac{\partial q_r}{\partial y}+\frac{Q}{\rho c_p}(T-T_\infty) \quad (3)$$

$$u\frac{\partial C}{\partial x}+v\frac{\partial C}{\partial y}=D\frac{\partial^2 C}{\partial y^2}-Kr(C-C_\infty) \quad (4)$$

Where u, v are the velocity components in the x and y directions, ν_f is the kinematic viscosity, ρ is the fluid density, B_0 is the transverse magnetic field, σ is the electrical conductivity of the fluid, α is the ratio of relaxation and retardation times, λ_1 is the relaxation time, T is the temperature of the fluid, k_f is the thermal conductivity of the fluid, c_p is the specific heat, T_∞ is the constant temperature of the fluid far away from the sheet, γ is the chemical reaction parameter, D is the diffusion coefficient, C and C_∞ are the species concentration and far away from the wall respectively.

The boundary conditions are

$$u=U_\omega(x)+L\frac{\partial u}{\partial y}, v=0, T=T_\omega=T_\infty+A_1\left(\frac{x}{l}\right)^m,$$

$$C=C_\omega=C_\infty+A_2\left(\frac{x}{l}\right)^m, \text{at } y=0$$

$$u\to 0, \frac{\partial u}{\partial y}\to 0, T\to T_\infty, C\to C_\infty \text{ as } y\to\infty \quad (5)$$

Where $U_\omega(x)=cx$ is the velocity of the stretching sheet, c is the proportionality constant of the stretching velocity, A_1 is the constant that depends on the temperature of the fluid, T_ω is the temperature of the stretching sheet, m is the surface temperature parameter, l is the characteristic length, A_2 is the constant that depends on the concentration of the fluid and C_ω is the species concentration at the wall.

To solve Eqs. (2)-(4), we introduce the following similarity transformations

$$\eta=\sqrt{\frac{c}{\nu_f}}y, u=cxf'(\eta), v=-\sqrt{c\nu_f}f(\eta), \theta(\eta)=\frac{T-T_\infty}{T_\omega-T_\infty}, \phi(\eta)=\frac{C-C_\infty}{C_\omega-C_\infty} \quad (6)$$

By the Rosseland diffusion approximation, the radiative heat flux q_r is given by

$$q_r=-\frac{4\sigma^*}{3k^*}\frac{\partial T^4}{\partial y} \quad (7)$$

The mean absorption coefficient of Rosseland and the Stefan-Boltzmann constant are denoted by k^* and σ^* respectively. By assuming the temperature differences within the flow are sufficiently small, so that T^4 can be described as a linear function of temperature.

$$T^4\approx 4{T_\infty}^3-3{T_\infty}^4 \quad (8)$$

Using (7) and (8) in equation (3), we obtain

$$\frac{\partial q_r}{\partial y}=-\frac{16\sigma^* {T_\infty}^3}{3k^*}\frac{\partial^2 T}{\partial y^2} \quad (9)$$

Applying the similarity variables, the governing Eqs.(2)-(4) are transformed into the non-linear ordinary differential equationas follows:

$$f'''+(1+\alpha)(ff''-f'^2)+Db(f''^2-ff'''')-(1+\alpha)Mf'=0 \quad (10)$$

$$\left(1+\frac{4R}{3}\right)\theta''+Pr(f\theta'-mf'\theta+\delta\theta)=0 \quad (11)$$

$$\phi''+Sc(f\phi'-mf'\phi-\gamma\phi)=0 \quad (12)$$

With boundary conditions

$$f(\eta)=0, f'(\eta)=1+Af''(\eta), \theta(\eta)=1, \phi(\eta)=1, \text{at } \eta=0,$$

$$f'(\eta)=0, f''(\eta)=0, \theta(\eta)=0, \phi(\eta)=0 \text{ as } \eta\to\infty \quad (13)$$

Where the governing parameters are defined as: $Db=\lambda_1 c$ is the Deborah number, $M=\frac{\sigma {B_0}^2}{b\rho_f}$ is the magnetic field parameter, $Pr=\frac{\mu c_p}{k_f}$ is the Prandtl number, $R=\frac{4\sigma^* {T_\infty}^3}{k^* k_f}$ is the radiation parameter, $\delta=\frac{Q}{\rho c_p c}$ is the heat source/sink parameter, $Sc=\frac{\nu_f}{D}$ is the Schmidt number, and $\gamma=\frac{Kr\delta^2}{\nu_f}$ is the chemical reaction parameter. The concentration, temperature, and dimensionless velocity are represented by ϕ, θ, and f, respectively, η is the similarity variable and prime denotes its differentiation with respect to η, A is the velocity slip parameter.

The other quantities that are described on the study are coefficient of skin friction C_f, the heat transfer rate $Nu_x$and the Sherwood number Sh_xwhich are defined as:

$$\left.\begin{aligned} {Re_x}^{\frac{1}{2}}C_f&=\frac{1}{1+\alpha}\left(f''(0)+Dbf''(0)\right),\\ Nu_x{Re_x}^{-\frac{1}{2}}&=-\theta'(0)\left(1+\frac{4R}{3}\right),\\ Sh_x{Re_x}^{-1/2}&=-\phi'(0)\end{aligned}\right\} \quad (14)$$

3. Solution by OHAM

To solve the above equations, we apply the basic principles and procedures of OHAM as it was developed by [27]. Thus, using the above principles the resolution of Eqs. (10)-(12) with respect to the corresponding boundary conditions (13) can be obtained using Optimal Homotopy Asymptotic Method as:

$$\left.\begin{aligned}(1-p)(f''+f')-H_1(p)\left[\left(f'''+(1+\alpha)(ff''-f'^2)+Db\left(f''^2-ff''''\right)-(1+\alpha)Mf'\right)-(f''+f')\right]=0,\\(1-\mathrm{p})(\theta'+\theta)-H_2(p)\left[\left(\left(1+\tfrac{4R}{3}\right)\theta''+Pr(f\theta'-mf'\theta+\delta\theta)\right)-(\theta'+\theta)\right]=0\\(1-\mathrm{p})(\phi'+\phi)-H_3(p)\left[\left(\phi''+Sc(f\phi'-mf'\phi-\gamma\phi)\right)-(\phi'+\phi)\right]=0\end{aligned}\right\} \quad (15)$$

When the embedding parameter$p=0$ and $p=1$

$$\psi(\eta,0)=V_0(\eta) \text{ and } \psi(\eta,1)=V(\eta) \quad (16)$$

Thus as p increases from 0 to 1, the solution varies from $V_0(\eta)$ to $V(\eta)$. For $p=0$ we can write

$$L(V_0(\eta))+g(\eta)=0, B(V_0)=0, \quad (17)$$

The auxiliary equation H(p) is chosen as:

$$H(p)=pC_1+p^2C_2+p^3C_3+\cdots, \quad (18)$$

Where $\mathrm{C}_1,\mathrm{C}_2,\mathrm{C}_3$ ... are constants which we call them convergence control parameters. Equally, the auxiliary equations for the momentum, heat transfer and mass transfer may be written as of (17) as:

$$\left.\begin{aligned}H_1(p)=pC_{11}+p^2C_{12}+\cdots\\H_2(p)=pC_{21}+p^2C_{22}+\cdots\\H_3(p)=pC_{31}+p^2C_{32}+\cdots\end{aligned}\right\} \quad (19)$$

Expanding $\psi(\eta,\mathrm{p})$ in series with respect to p one can write:

$$\psi(\eta,p,C)_i=V_0(\eta)+\textstyle\sum_{k\geq1}V_k(\eta,C_i)p^k, i=1,2,3\ldots \quad (20)$$

Now following the method and substituting (19) in to (15) we can write:

The Zero[th] order as:

$$\left.\begin{aligned}p^0: f''_0+f'_0=0\\f_0(0)=S, f'_0(0)=1+Af''_0(0),\\\theta'_0+\theta_0=0\\\theta_0(0)=1,\\\phi'_0+\phi_0=0\\\phi_0(0)=1,\end{aligned}\right\} \quad (21)$$

Based on the corresponding boundary conditions one can find the Zero[th] order solution as

$$\left.\begin{aligned}f_0(\eta)=\frac{e^{-\eta}(-1+e^{\eta})}{1+A},\\\theta_0(\eta)=e^{-\eta},\\\phi_0(\eta)=e^{-\eta}\end{aligned}\right\} \quad (22)$$

In the same way, we can find the first and second order solutions too. Hence, solutions for the momentum, heat transfer, and mass transfer equation (up to second-order terms) are given by

$$\left.\begin{aligned}f(\eta)=f_0(\eta)+f_1(\eta)+f_2(\eta)\\\theta(\eta)=\theta_0(\eta)+\theta_1(\eta)+\theta_2(\eta)\\\phi(\eta)=\phi_0(\eta)+\phi_1(\eta)+\phi_2(\eta)\end{aligned}\right\} \quad (23)$$

On substituting the values of $f(\eta)$, $\theta(\eta)$ and $\phi(\eta)$ from (23) in to equations (10),(11) and (12), we can find residuals as

$R_1(\eta,C_{11},C_{12}), R_2(\eta,C_{21},C_{22})$ and $R_3(\eta,C_{31},C_{32})$, afterward, we can obtain the Jacobians $J_1, J_2,$ and J_3 as follows:

$$J_1(\eta,C_{11},C_{12})=\textstyle\int_0^b {R_1}^2(\eta,C_{11},C_{12})d\eta \quad (24)$$

$$J_2(\eta,C_{21},C_{22})=\textstyle\int_0^b {R_2}^2(\eta,C_{21},C_{22})d\eta \quad (25)$$

$$J_3(\eta,C_{31},C_{32})=\textstyle\int_0^b {R_3}^2(\eta,C_{31},C_{32})d\eta \quad (26)$$

Where the residuals

$$R_1(\eta,C_{11},C_{12})=f'''+(1+\alpha)(ff''-f'^2)+Db(f''^2-ff'''')-(1+\alpha)Mf',$$

$$R_2(\eta,C_{21},C_{22})=\left(1+\tfrac{4R}{3}\right)\theta''+Pr(f\theta'-mf'\theta+\delta\theta),$$

$$R_3(\eta,C_{31},C_{32})=\phi''+Sc(f\phi'-mf'\phi-\gamma\phi)$$

In order to solve the optimal values of the parameters $C_{11},C_{12},C_{21},C_{22},C_{31},and\ C_{32}$, we apply,

$$\frac{\partial J_1}{\partial C_{11}}=\frac{\partial J_1}{\partial C_{12}}=0, \frac{\partial J_2}{\partial C_{21}}=\frac{\partial J_2}{\partial C_{22}}=0, \text{and } \frac{\partial J_3}{\partial C_{31}}=\frac{\partial J_3}{\partial C_{32}}=0.$$

Using these constants which we call it convergence control parameters, the approximate solution of the problem (to order m) can be determined very easily.

4. Results

To study the flow model for the above coupled non-linear ordinary differential equations (10)-(12) an Optimal Homotopy Asymptotic Method has been employed. The obtained results are displayed through graphs figures. 2-16. To check how much this method is accurate, it is compared the rate of heat transfer with the results done by Narayana [17] and Chen [30] for different values of m and we got it in a good agreement as shown in Table 1. It is also watched that the raise of (Db) enlarges the local Nusselt number.

Table 1. *Comparison of local Nusselt number* $-\theta'(0)$ *for various values of m, when* $R=\alpha=0$, $Db=0$, $M=\delta=0.A=0$ *and* $Pr=1$.

m	Chen[30]	Narayana[17]	Present
0	0.58199	0.5820	0.585319
1	-	1.0000	1.0000
2	1.33334	1.3333	1.33334

Figure. 2 and 3 demonstrate the influence of the Deborah number (Db) on the velocity and temperature profile in the presence of velocity slip parameter. The velocity profile of the fluid increases when the Deborah number(Db) increases, since there is a direct proportionality between Deborah number (Db) and the stretching sheet rate $(Db=\lambda_1 c)$. Increasing(Db) results in a higher motion of the fluid in the boundary layer especially adjacent to the surface sheet.

However, the distribution of fluid temperature decreases when the Deborah number (Db) increases. It is because (Db) is proportional to the retardation time, which increases with an increase of the retardation time. As a consequence, the thickness of thermal boundary layer becomes weak with an increase of the retardation time.

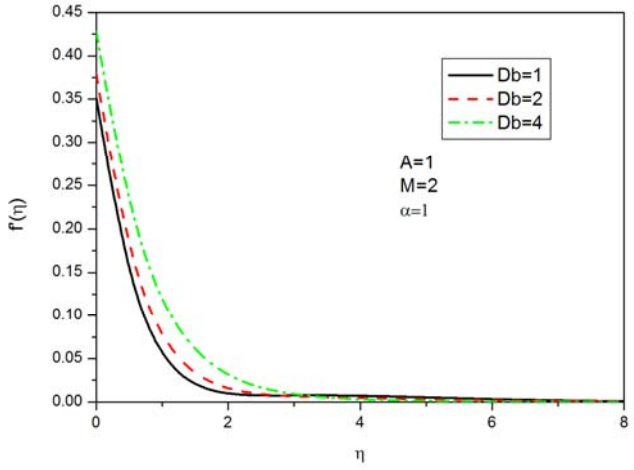

Figure 2. *Velocity profile for different values of Db.*

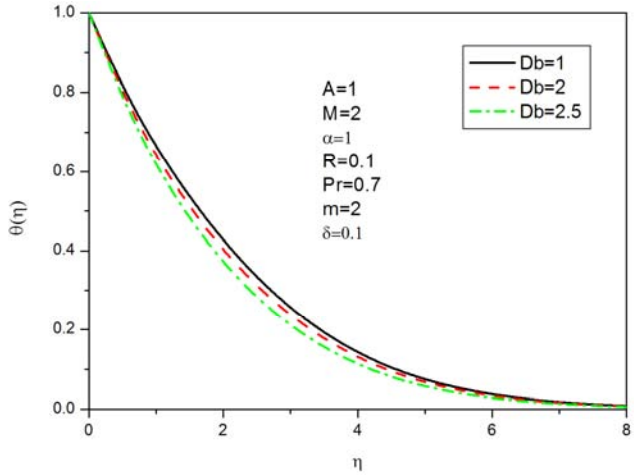

Figure 3. *Temperature profile for differentvalues of Db.*

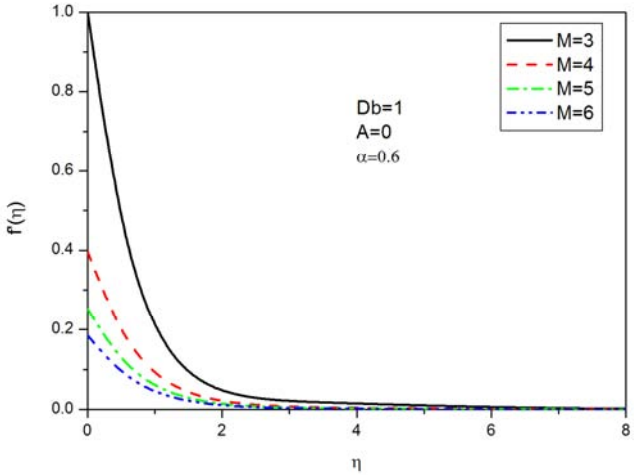

Figure 4. *Velocity profile for different values of M.*

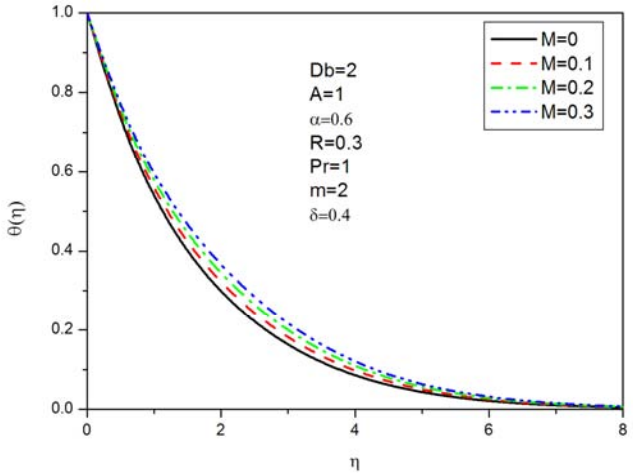

Figure 5. *Temperature profile for different values of M.*

Figures.4 and 5 display the magnetic field parameter (M) effect on the velocity and temperature profile. The magnetic field parameter (M) has opposite effects on the velocity and temperature profiles. Increasing the values of (M)decreases the velocity profile. It is because, a Lorentz force created due to the presence of magnetic field which arises by drag force. This force reduces the movement of the fluid. This shows that increasing (M) increases the retarding force and accordingly the velocity lessens. In the case of temperature the increase of (M) increases the temperature profile, physically the magnetic field retards the velocity profile which in turn induces the temperature field that results in an increase of the temperature profiles. Hence, to manage the flow characteristics the magnetic field can be used. The ratio of relaxation and retardation times(α) effect on the distribution of velocity is presented by figure 6. The result has shown that, the velocity profile decreases when (α) increases. This indicates that, a rise in (α) decrease in fluid retardation time which results to stop the rushing of fluid motion.

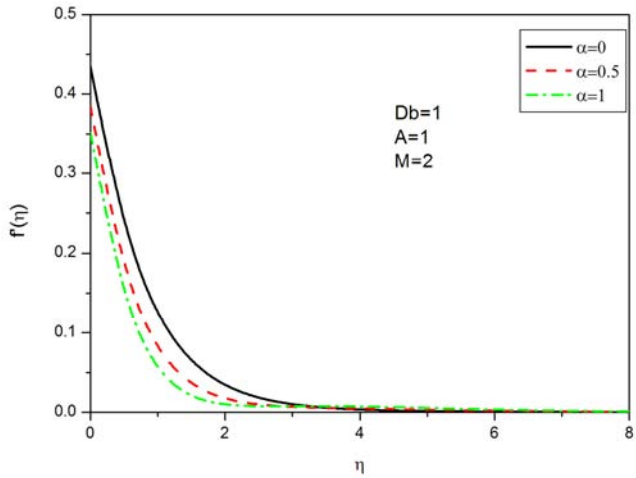

Figure 6. *Velocity profile for different values of a.*

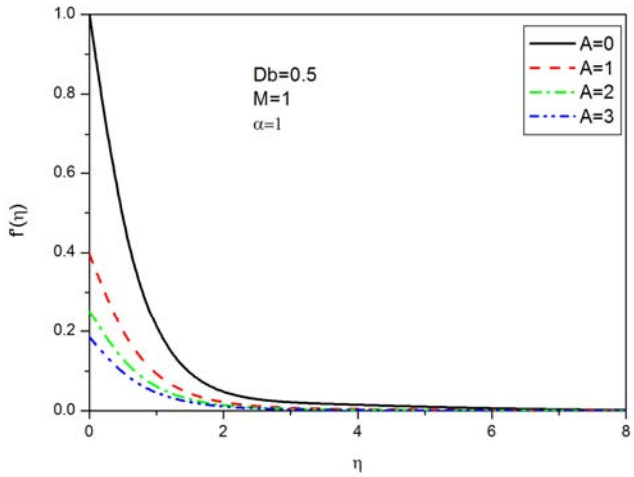

Figure 7. *Velocity profile for different values of* A.

The pressure velocity slip parameter (A) on the velocity field is illustrated in figure 7. It is distinguished that, this parameter has an opposing effect on the velocity profile of the fluid. Figure 8 portrays the impact of the Prandtl number (Pr) on the circulation of temperature. From the figure, it is observed that increasing the values of (Pr) decreases the temperature profile. The main cause is that (Pr) depends on the thermal diffusivity. Thus the weakness of thermal diffusivity is due to large Prandtl number for which the temperature to be lower and the thermal boundary layer thickness thinner. Figure 9 illustrates the influence of the heat sink parameter $(\delta < 0)$ on the temperature profile. The heat sink makes the temperature of the fluid to decrease. It is because, the energy contained in the boundary layer is absorbed by the heat sink, that makes the fluid temperature to decrease.

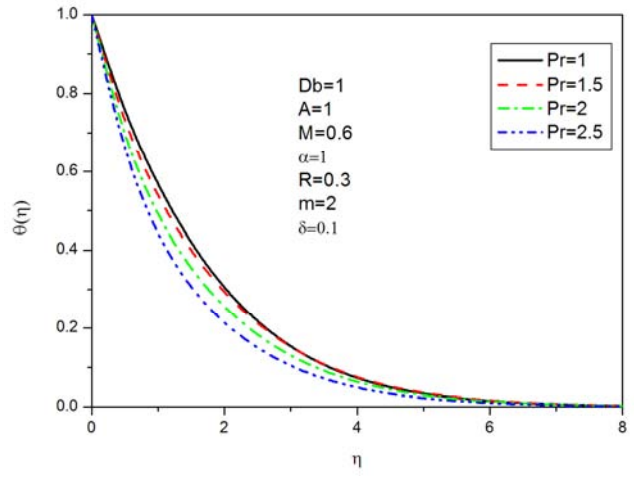

Figure 8. *Temperature profile for different values of* Pr.

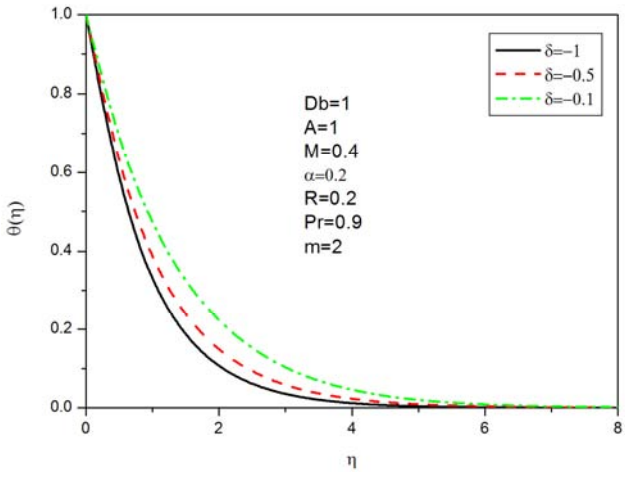

Figure 9. *Temperature profile for different values of* δ.

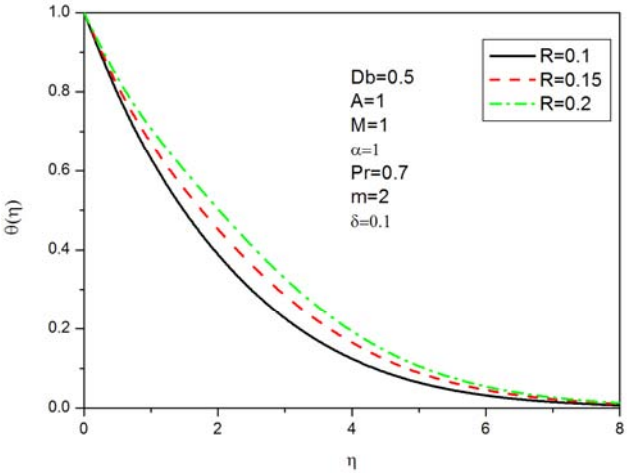

Figure 10. *Temperature profile for different values of* R.

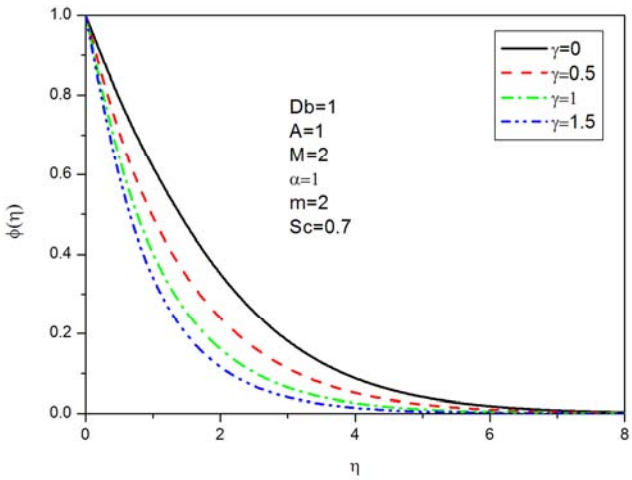

Figure 11. *Concentration profile for different values of* γ.

Radiation parameter (R) effect on the distribution of temperature is demonstrated by figure 10. It is watched that the increase of the thermal radiation parameter (R) increases the temperature profile. Hence, it makes the cooling process to proceed at a faster rate. Figure 11 illustrates the influence of chemical reaction parameter (γ) on the concentration

profiles. It is indicated that an increase of (γ) decreases the concentration profile, physically, increasing the chemical reaction parameter produces a decrease in the species of concentration and boundary layer thickness.

The concentration profile due to an effect of Schmidt number (Sc) is displayed by figure 12.The result has shown that, an increase in (Sc) decreases the concentration profile, physically, (Sc) increases means the molecular diffusion decreases. Hence, the concentration of the species is higher for small values of (Sc) and lower for larger values of (Sc). Figure 13 displays the consequence of surface temperature parameter (m) on the concentration profile. The result has shown that, when the values of (m) increases, the concentration profile decreases. This is because the fluid flow is caused by stretching of the sheet and the stretching sheet of concentration is greater than the free stretch concentration (i.e.$C_\omega > C_\infty$).

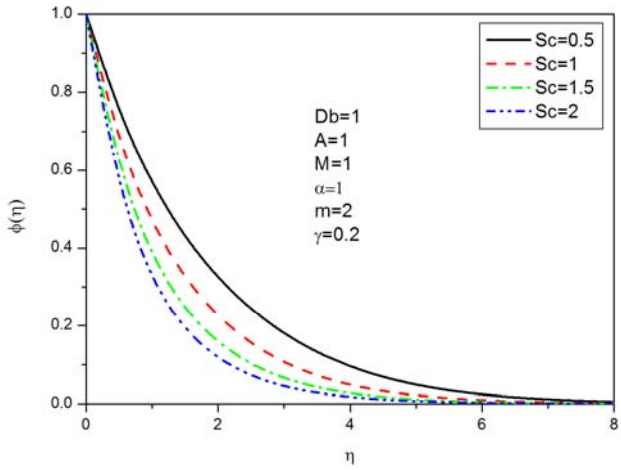

Figure 12. *Concentration profile for different values of Sc.*

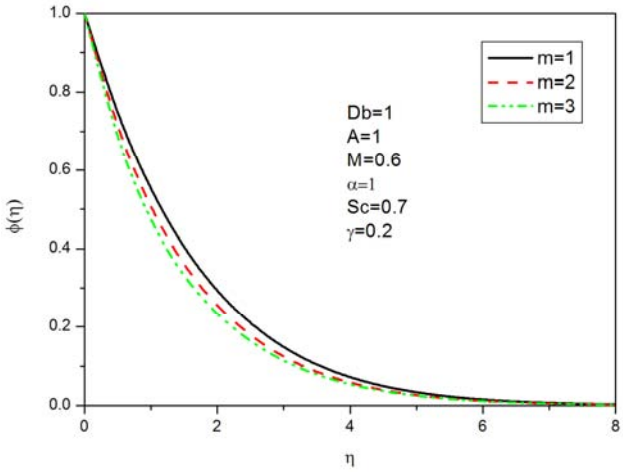

Figure 13. *Concentration profile for different values of m.*

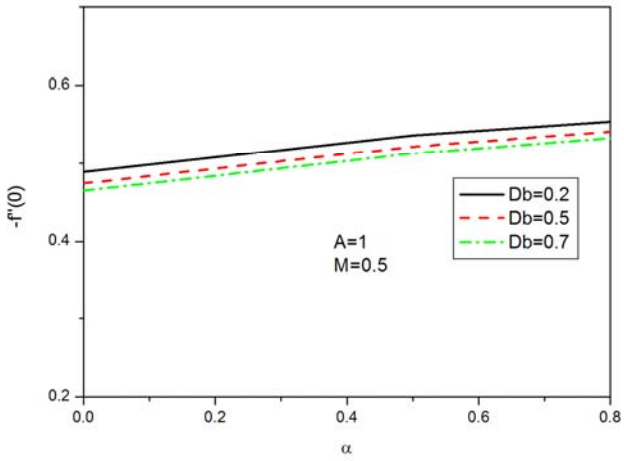

Figure 14. *Skin friction coefficient for different values of Db & α.*

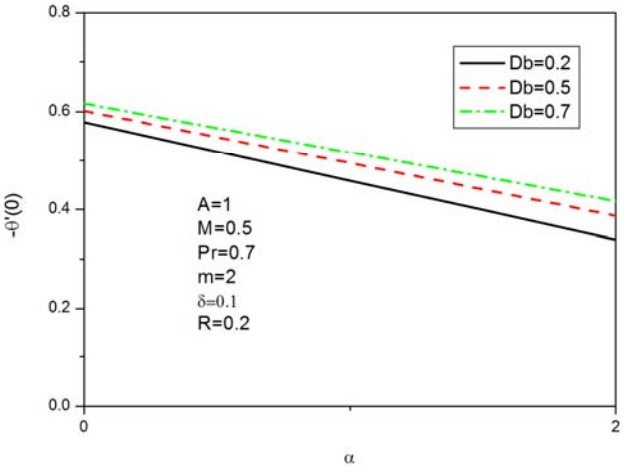

Figure 15. *Nusselt number for different values of Db & α.*

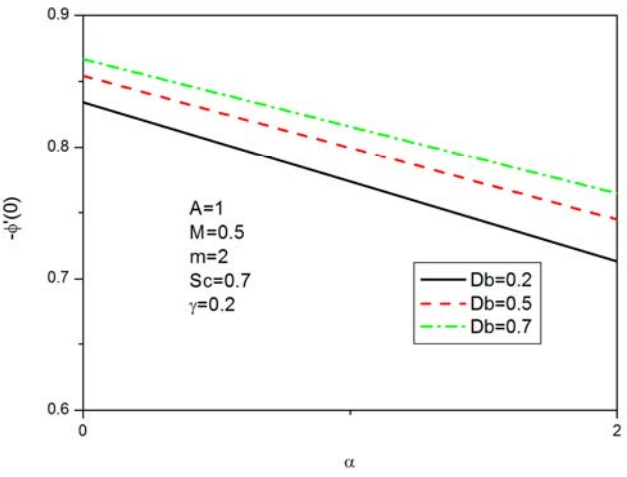

Figure 16. *Sherwood number for different values of Db & α.*

The variation of coefficient of skin friction, Nusselt number, and Sherwood number for diverse values of (α) and (Db) is displayed in figures. 14, 15 and 16. The result has shown that, when(α) increases, the coefficient of skin friction increases, while the rate of heat transfer and Sherwood number decreases. And when the values of the

Deborah number (Db) increases, the coefficient of skin friction decreases, the rate of heat transfer and Sherwood number increases.

5. Discussions

The endeavor of this analysis is to investigate an MHD fluid flow of steady, laminar two-dimensional heat and mass transport of a Jeffery fluid on a stretching sheet. The outcome of velocity slip on the fluid flow is incorporated. To compute the solutions of the governing problem it is applied an analytic method named optimal homotopy analysis method (OHAM). Therefore, for diverse values of the dimensionless parameters velocity profile, temperature profile, concentration profile and as well as the coefficient of skin friction, the heat transport rate and mass transport rate are evaluated. It is acquired that,the velocity slip parameter (k) and the Deborah number (β) have reverse impacts on the velocity distributions of the fluid flow. However, the effects of heat source parameter (δ) and thermal radiation parameter (R) on the temperature profile is similar. The accuracy of this analytic technique is checked by comparing the Nusselt number with the formerly published works and the results are found to be in excellent agreement. In addition, as to the author's knowledge, the study of slip velocity effect on an MHD Jeffery fluid flow and the transfer characteristics heat and mass is not enough. Especially, several problems were not solved analytically. Based on the above reasons, the study of this problem is very valid.

6. Conclusions

In this article, it is considered a steady, laminar, two-dimensional MHD Jeffery fluid flow with heat source. The temperature and concentration are assumed to be in the form of power low and the problem is solved analytically.

The results obtained in the study are summarized as follows:

1) When the values of (Db) increases, the fluid velocity increases while the temperature profile decreases.
2) Magnetic field parameter has an inverse effect on the velocity profile and temperature. The velocity profile decreases with an increase of (α).
3) The velocity profile reduces with an increase of slip velocity.
4) The distribution of temperature decreases with an increase of (Pr) and increases with an increase of $(R)$and (δ).
5) The effect of the Schmidt number and chemical reaction is to decrease the concentration profile.
6) An increase in (m) makes to decrease the concentration profile.
7) The coefficient of skin friction increases with an increase of (α) while the Nusselt number and Sherwood number decreases.
8) The coefficient of skin friction decreases with an increase of (Db) while the Nusselt number and Sherwood increases.

References

[1] B. C. Sakiadis, "boundary layer surface on continuous solid surface: L Boundary layer equations for two dimensional and ax symmetric flow," J Am Inst Chem.Eng, 1961, 7: 26–8.

[2] L.J. Crane, "Flow past a stretching plate," *Z Angew Math Phys*, 1970, 21:645–647.

[3] B.Dutta, P. Roy, and A. Gupta, "Temperature field in the flow over a stretching sheet with uniform heat flux," Int. J Commun. Heat.MassTransf, 1985, 12: 89–94.

[4] P. Gupta and A. Gupta, "Heat and mass transfer on a stretching sheet with suction or blowing," Can.J.Chem. Eng, 1977,55: 744–746.

[5] C. Chen and M. Char, "Heat transfer of a continuous stretching surface with suction or blowing," J.Math.Anal. Appl, 1988, 135: 568–580.

[6] M. Salleh, R. Nazar, and I. Pop, "Boundary layer flow and heat transfer over a stretching sheet with Newtonian heating," J. Taiwan Inst. Chem. Eng.,2010, 41: 651–655.

[7] P. Babu, J.A. Rao, and S. Sheri, "Radiation Effect on Mhd Heat and Mass Transfer Flow over a Shrinking Sheet with Mass Suction," J. Appl. Fluid Mech., 2014, 7(4): 641–650.

[8] N. S. Akbar, S. Nadeem, R.U. Haq, and Z.H. Khan, "Radiation effects on MHD stagnation point flow of nanofluid towards a stretching surface with convective boundary condition," Chin J Aeronaut, 2013, 26: 1389–97.

[9] B. C. Rout and S. R. Mishra, "Thermal energy transport on MHD nanofluid flow over a stretching surface: A comparative study," Eng. Sci. Technol. an Int. J., 2018, 21: 60–69.

[10] N. S. Akbar, S. Nadeem, R. U. Haq, and Z. H. Khan, "Dual solutions in MHD stagnation point flow of a Prandtl fluid impinging on a shrinking sheet," Appl Math Mech, 2014, 35: 813–20.

[11] O. D. Makinde and S. R. Mishra, "On Stagnation Point Flow of Variable Viscosity Nanofluids Past a Stretching Surface with Radiative Heat," Int. J. Appl. Comput. Math., 2017, 3: 561-578

[12] D. Pal and G. Mandal, "Influence of Lorentz Force and Thermal Radiation on Heat Transfer of Nanofluids Over a Stretching Sheet with Velocity–Thermal Slip," Int. J. Appl. Comput. Math., 2017, 3(4): 3001-3020.

[13] D. Pal and N. Roy, "Influence of Brownian Motion and Thermal Radiation on Heat Transfer of a Nanofluid Over Stretching Sheet with Slip Velocity," Int. J. Appl. Comput. Math,2017, 3(4): 3355–3377.

[14] Y. S. Daniel, Z. A. Aziz, Z. Ismail, and F. Salah, "Effects of slip and convective conditions on MHD flow of nanofluid over a porous nonlinear stretching/shrinking sheet," Aust. J. Mech. Eng., 2017.

[15] M. Sheikholeslami, H.. Ashorynejad, D.. Ganji, and A. Kolahdooz, "Investigation of rotating MHD viscous flow and heat transfer between stretching and porous surfaces using analytical method," Math probl Eng, 2011: 1–17.

[16] G. Adamu and B. Shankar, "MHD Flow of Non-Newtonian Viscoelastic Fluid on Stretching Sheet With The Effect of Slip Velocity," Int. J. Eng. Manuf. Sci., 2018, 8(1): 1–14.

[17] P. V. S. Narayana and D. H. Babu, "Numerical study of MHD heat and mass transfer of a Jeffrey fluid over a stretching sheet with chemical reaction and thermal radiation," J. Taiwan Inst. Chem. *Eng.*,2016,59: 18–25.

[18] K. Ammad and A. Ishak, "Magnetohydrodynamic (MHD) Jeffrey fluid over a stretching vertical surface in a porous medium," Propuls. Power Res., 2017, 6(4): 269–276.

[19] M. Qasim, "Heat and mass transfer in a Jeffrey fluid over a stretching sheet with heat source/sink," Alex Eng J, 2013, 52: 571–575.

[20] K. Das, N. Acharya, and P.. Kundu, "Radiative flow of MHD Jeffrey fluid past a stretching sheet with surface slip and melting heat transfer," Alexandria Eng. J., 2015, 54: 815–821.

[21] A. Zeeshan and A. Majeed, "Heat transfer analysis of Jeffery fluid flow over a stretching sheet with suction/injection and magnetic dipole effect," Alexandria Eng. J., 2016, 55: 2171–2181.

[22] S. Nadeem, R. Mehmood, and N. Akbar, "Non orthogonal stagnation point flow of a nano non-Newtonian fluid towards a stretching surface with heat transfer," Int. J. Heat.Mass Transf., 2013, 57: 679–689.

[23] S. Nadeem, Noreen, and S. Akbar, "Peristaltic flow of a Jeffrey fluid with variable viscosity in an asymmetric channel,",Z. Natur schung A, 2009,64a: 713–722.

[24] M. Khan, F. Iftikhar, and A. Anjum, "Some unsteady flows of a Jeffrey fluid between two side walls over a plane wall," Z.Natur sch, 2011, 66: 745–752.

[25] T. Hayat, S. Asad, M. Qasim, and A. Hendi, "Boundary layer flow of a Jeffrey fluid with convective boundary conditions," Int. J.Numer. Methods Fluids, 2012, 69AD: 1350–1362.

[26] T.Hayat, S.. Shehzad, M. Qasim, and S. Obaidt, "Thermal radiation effects on the mixed convection stagnation-point flow in a Jeffery fluid," Z. Natur sch, 2011, 66: 606–614.

[27] V.Marinca, N. Herisan, C. Bota, and B. Marinca, "An optimal homotopy asymptotic method applied to the steady flow of fourth-grade fluid past a porous plate," Appl Math Lett, 2009, 22: 245–251.

[28] T.Hayat, S.. Shehzad, M. Qasim, and S. Obaidat, "radiative flow of Jeffery fluid in a porous medium with power law heat flux and heat source," Nucl Eng, 2012, 243: 15–19.

[29] M.Qasim, "Heat and mass transfer in a Jeffrey fluid over a stretching sheet with heat source/sink," Alexandria Eng. J., 2013, 52: 571–575.

[30] C. H. Chen, "Laminar mixed convection adjacent to vertical continuously stretching sheets," *Heat Mass Transf.*, 1998, 33: 471–476.